TASK QUARTERLY 12 No 3, 135–145

AERODYNAMIC RESEARCH ON THE MIDSECTION OF A LONG TURBINE BLADE

DAVID ŠIMURDA[1], MARTIN LUXA[1], PAVEL ŠAFAŘÍK[2] AND JAROSLAV SYNÁČ[3]

[1]*Institute of Thermomechanics, AS CR, v.v.i., Dolejškova 5, 18200 Praha, Czech Republic*
simurda@it.cas.cz, luxa@it.cas.cz

[2]*Faculty of Mechanical Engineering, CTU Prague, Technická 4, 16607 Praha, Czech Republic*
pavel.safarik@fs.cvut.cz

[3]*ŠKODA POWER a.s., Tylova 1/57, 30128 Plzeň, Czech Republic*
jaroslav.synac@skoda.cz

(Received 30 April 2008)

Abstract: The paper is concerned with experimental aerodynamic research on the midsection of a 1220 mm long turbine rotor blade. Optical as well as pneumatic measurements of the midsection blade cascade have been performed in a suction type high-speed wind tunnel. The results of measurements are analyzed and discussed.

Interferograms and schlieren pictures taken in a wide range of isentropic exit Mach numbers and incidence angles exhibit the existence of several phenomena occurring in the transonic flow field at certain conditions concerning the exit Mach number and the angle of incidence. A flow separation taking place at an extreme negative incidence has been found to produce an additional loss of 6%. The presence of the reflection of an exit shock wave on the suction side of the neighbouring profile has been found to have a substantial influence on the losses, since the loss coefficient value has increased about 10% in cases without the reflection, *i.e.* the cases at a high exit Mach number and a high positive angle of incidence. Several reflection types have been observed and described.

Keywords: transonic flow, turbine blade cascade, experimental research

Notation

AR – aspect ratio [–]
a^* – critical sound velocity [m/s]
b – chord [m]
b_x – axial chord [m]
c – flow velocity [m/s]

Ma – Mach number [–]
Ma^* – c/a^* [–]
o – throat opening [m]
p – pressure [Pa]
s – pitch [m]
t – profile thickness [m]
w – relative velocity [m/s]
α – flow angle [°]
γ – stagger angle [°]
ι – incidence angle [°]
ζ – kinetic energy loss coefficient [–]

Subscripts

des – design value
is – isentropic
TE – trailing edge
1 – inlet value
2 – exit value

1. Introduction

The experimental data obtained in transonic flow fields in turbine blade cascades forms an important basis for designing, studying and operating turbomachines. This data provides information on the behaviour of a compressible fluid in the high-speed conditions occurring in the last stages of steam turbines with a large output. Most attention has to be paid to the flow structures that have a strong influence on the loss of kinetic energy and hence on the efficiency. The intensity of such structures increases with the increasing radial distance from the hub due to the higher circumferential velocity.

The midsection is located at a radius of 1150 mm right above a special type of a damping device in the middle part of the blade (Figure 1). The design incidence and the exit Mach number of the midsection are $\iota = 0°$ and $\mathrm{Ma}_{2\mathrm{is}} = 1.323$, respectively. The velocity triangles in Figure 1 illustrate the situation at the inlet and outlet of such midsection.

2. Experiment

The experimental results were obtained by means of measurements in a suction-type wind tunnel at the Institute of Thermomechanics AS CR. The blade cascade consisted of 6 prismatic blades. The basic geometry and characteristic dimensions of the blade cascade are shown in Figure 2 and Table 1, respectively.

The measurement setup scheme is shown in Figure 3. Optical interferometric measurements set up for an infinite fringe [1] were performed in the range of exit Mach numbers of $0.5 \leq \mathrm{Ma}_{2\mathrm{is}} \leq 1.5$ and the incidence angles of $-30° \leq \iota \leq +30°$; the Reynolds number related to the profile chord b and the isentropic exit Mach number $\mathrm{Ma}_{2\mathrm{is}}$ were in the range from $\mathrm{Re} = 5 \cdot 10^6$ to $\mathrm{Re} = 12.8 \cdot 10^6$. Interferograms were used for evaluating the distribution of nondimensional velocity $\mathrm{Ma}^*_{\mathrm{is}}$ along the profiles. In

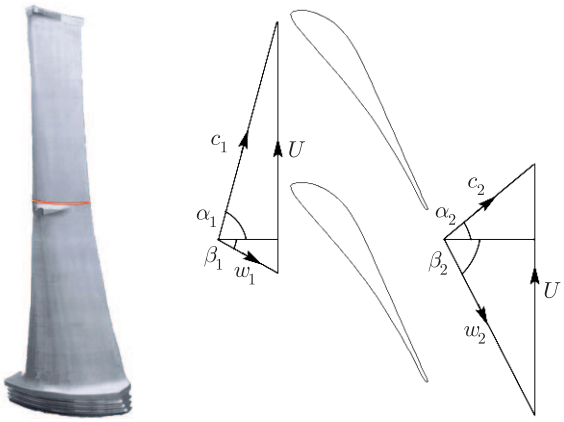

Figure 1. 1220 mm long blade of the last rotor stage, with velocity triangles

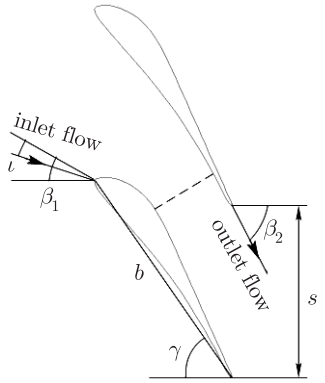

Figure 2. Scheme of the blade cascade geometry

Table 1. Characteristic dimensions of the blade cascade

Pitch/Chord	s/b	0.718
Max. Thickness/Chord	t/b	0.13
Aspect Ratio	AR	1.6
Throat Opening/Chord	o/b	0.28
Stagger Angle	γ	54.8°
Trailing Edge Thickness/Chord	t_{TE}/b	0.0073
Design Inlet Flow Angle	$\beta_{1\mathrm{des}}$	−29.1°
Design Incidence	ι_{des}	0°

addition to the interferograms, schlieren photographs providing a good qualitative picture of the transonic flow were taken in all conditions.

A traversing device with a five-hole conical probe which adjusts against the stream automatically was utilized for measuring the static and total pressure and the exit flow angle distributions at the traversing plane downstream of the blade cascade. Traversing was carried out in a range of incidence angles of $-30° \leq \iota \leq +30°$ and the exit Mach numbers of $0.5 \leq \mathrm{Ma}_{2\mathrm{is}} \leq 1.5$. The loss coefficient and exit flow angle

reference values in all conditions were evaluated using the data reduction method. This method is based on solving a set of equations consisting of all the conservation laws (mass, energy, momentum) and the equation of state of an ideal gas [2] for measured data and reduced values.

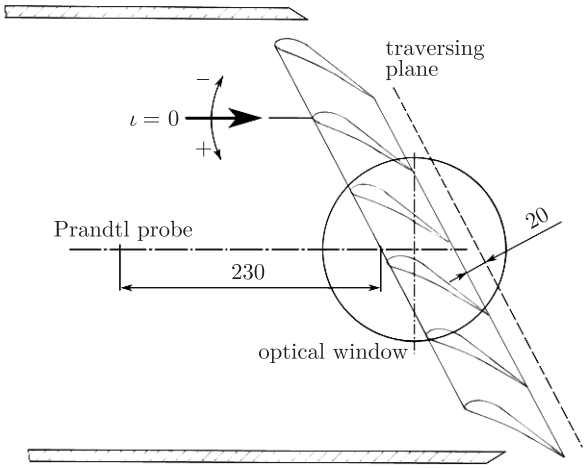

Figure 3. Scheme of the measurement setup

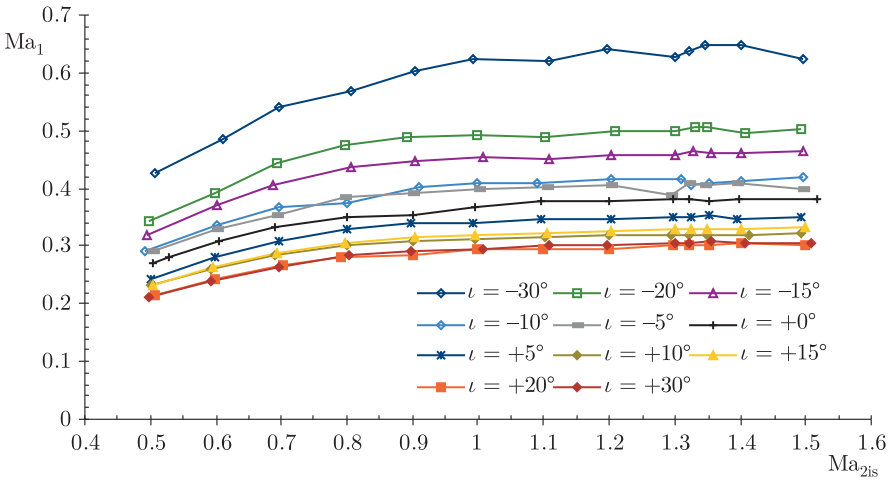

Figure 4. Cascade characteristics $\mathrm{Ma}_1 = f(\mathrm{Ma}_{2\mathrm{is}})$, $\iota = \mathrm{const}$.

3. Results and discussion

3.1. Inlet and leading edge

Figure 4 shows clearly that the inlet velocity has been subsonic in the whole range of exit Mach numbers. All the curves in Figure 4 embody a typical development. The inlet Mach number rises until aerodynamic choking takes place. Beyond the exit Mach number of aerodynamic choking the mass flow through the blade cascade remains constant and the inlet velocities do not change significantly. A variation of the inlet Mach number beyond $\mathrm{Ma}_{2\mathrm{is}} = 1$ can be observed in case of incidence

$\iota = -30°$. An interferogram taken at $\mathrm{Ma}_{2\mathrm{is}} = 1.35$ and $\iota = -30°$ (Figure 5) shows a large region of a separated flow right on the leading edge on the pressure side of the blade. The effective geometry of the interblade channel changes as a result of the separation, hence, the variation mentioned above embodies different behaviour. An uneven course of the $\iota = -30°$ variation probably results from the changing extent of the separation region under different conditions concerning the outlet/inlet pressure ratio. The increased sensitivity of the inlet Mach number upon the angle of incidence ι at negative incidences is a consequence of the decreasing inlet area A_1, which changes with the cosine of α_1. Therefore, the changes of A_1 at positive incidences ($\iota = +30°$, $\alpha_1 = -0.9°$) are very small. Similar behaviour has been observed and described in [3].

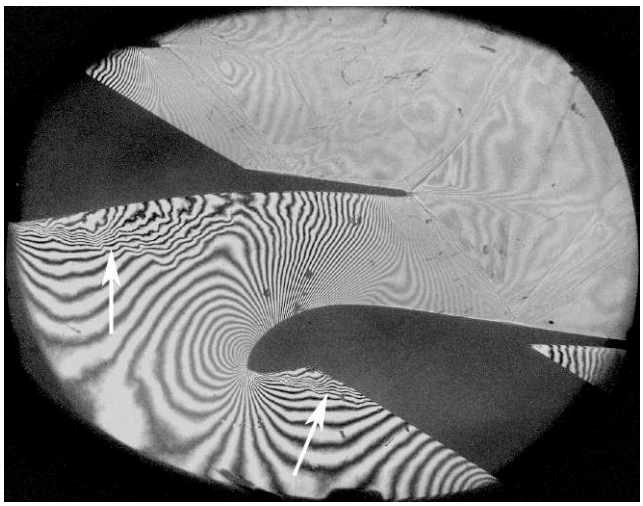

Figure 5. Interferogram taken at $\mathrm{Ma}_{2\mathrm{is}} = 1.35$, $\iota = -30°$, showing a flow separation

3.2. Interblade channel

An interferogram taken at $\mathrm{Ma}_{2\mathrm{is}} = 1.093$ and $\iota = -30°$ (Figure 6) clearly shows a local region of a decelerated flow on the profile's suction side. This so called "supersonic compression at transonic expansion" takes place close to a sonic line where the curved surface of the suction side verges into a straight surface. A sudden change of the surface curvature results in a reflection of the compression characteristics as shown in Figure 7. The expansion characteristics coming from the surface convex part reflect from the sonic line as compression characteristics. These reflected characteristics reflect again, this time from the straight surface, keeping their compression character. Therefore, the region of compression occurs between the point of change in the curvature and the first neutral characteristic. Hence, the compression region's extent depends on the sonic line shape. The distribution of $\mathrm{Ma}^*_{\mathrm{is}}$ along the profile's suction side (Figure 8) also confirms a drop of pressure at position $0.49 < x/b_x < 0.57$. A more detailed description can be found in [4].

3.3. Exit and trailing edge

An exit shock wave first appears at $\mathrm{Ma}_{2\mathrm{is}} = 0.9$ as a normal shock decelerating the supersonic flow which cannot be maintained by the exit/inlet pressure ratio. With

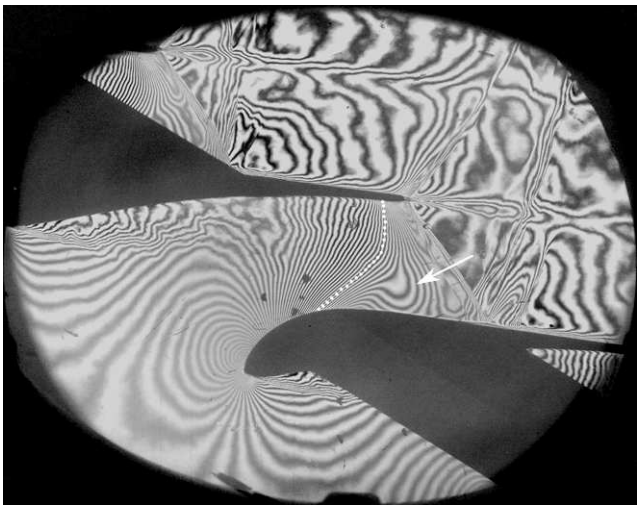

Figure 6. Interferogram taken at $Ma_{2is} = 1.093$, $\iota = -30°$, showing supersonic compression at transonic expansion and sonic line

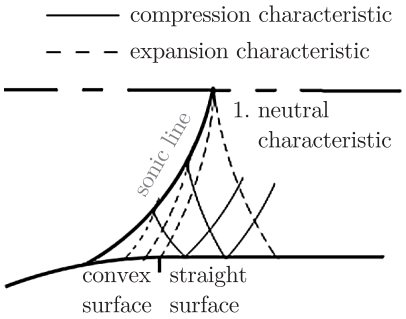

Figure 7. Scheme of compression region generation

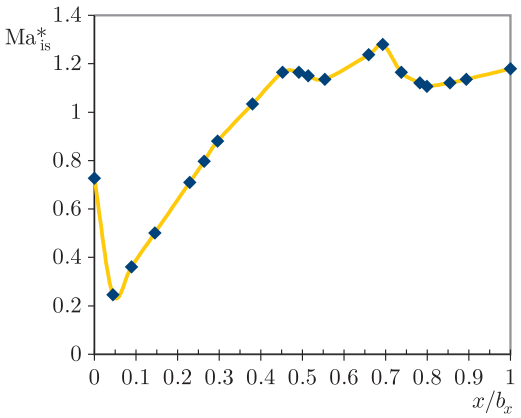

Figure 8. Distribution of Ma^*_{is} along suction surface of the blade. $Ma_{2is} = 1.093$, $\iota = -30°$

the increasing exit Mach number the shock wave develops into an oblique shock. It reflects from the suction side of the neighbouring blade. However, at the exit Mach number of 1.0 and the incidence of $\iota = -30°$an oblique shock wave cannot be formed

on reflection, so the incident shock wave becomes normal to the suction surface of the neighbouring profile, and a Mach reflection (Figure 9) occurs, as described for the example in [5]. As the exit Mach number continues to increase, the exit shocks obliqueness grows and the reflection point shifts downstream.

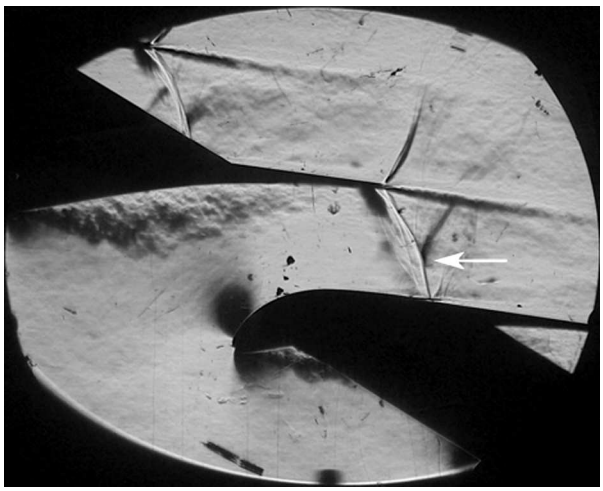

Figure 9. Schlieren picture taken at $\mathrm{Ma}_{2\mathrm{is}} = 0.998$, $\iota = -30^\circ$ showing Mach reflection

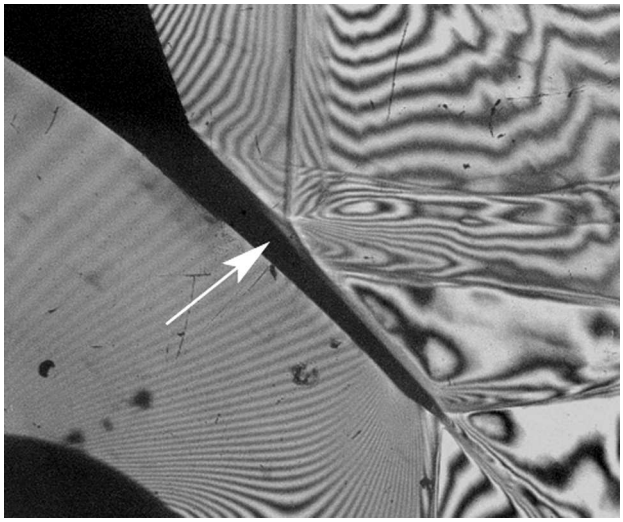

Figure 10. Interferogram taken at $\mathrm{Ma}_{2\mathrm{is}} = 1.327$, $\iota = +10^\circ$ showing a shock wave – laminar boundary layer interaction

Since the boundary layer on the suction surface of the blade is laminar we observe that two oblique shock waves generate upon reflection (Figure 10). The mechanism of this shock wave – laminar boundary layer interaction is sketched in Figure 11. A strong pressure gradient of the incident shock wave R_1 in a subsonic flow inside the boundary layer propagates upstream to point 0 causing the boundary layer separation at point S. A change of the free stream flow direction of the surface due to the boundary layer separation results in a generation of a system of weak compression

waves which eventually merge into a shock wave R_2. However, the Incident shock R_1 deflects the free stream flow at point D towards the surface, therefore the flow reattaches. A subsequent change of the flow direction results again in a generation of a system of compression waves merging into a closing shock wave R_3. A more detailed description can be found in [6]. The course of dimensionless velocity $\mathrm{Ma}^*_{\mathrm{is}}$ in the interaction region is well visible in Figure 12 at location $0.68 < x/b_x < 0.8$ and corresponds to the course of static pressure in the sketch (Figure 11). This interaction is always accompanied by a transition of the laminar boundary layer to turbulent. An increase in the boundary layer thickness behind the interaction in Figure 10 is evident. The shock wave – laminar boundary layer interaction has been observed at regimes with the exit Mach numbers of $\mathrm{Ma}_{2\mathrm{is}} \geq 1$ apart from those at the incidence of $\iota = +30°$ (Figure 13). In the latter case the boundary layer on the suction side has been already turbulent at the interaction location. The one missing regime at $\mathrm{Ma}_{2\mathrm{is}} = 1$ and $\iota = -30°$ (Figure 13) is the previously mentioned case of the Mach reflection. Regimes from the upper right corner of the graph in Figure 13 are missing, since the exit shock wave obliqueness is such that the shock completely misses the neighbouring blade, *i.e.* an overload regime occurs.

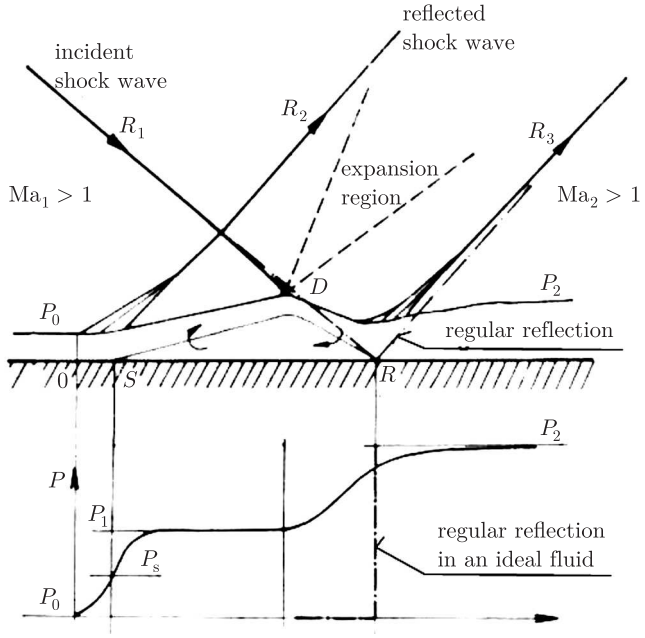

Figure 11. Sketch of a shock wave – laminar boundary layer interaction mechanism

In general, the exit flow angle values correspond to the blade cascade geometry till $\mathrm{Ma}_{2\mathrm{is}} = 1$ (Figure 14). Above this value supersonic deflection takes place and the exit flow angle values depend on the velocity conditions on both the pressure and suction sides near the trailing edge. A more significant decrease in the exit flow angle at higher exit Mach numbers and positive incidences probably results from the fact that the flow on the suction side is not decelerated by the exit shock wave whose obliqueness is such that the shock misses the neighbouring blade. Therefore,

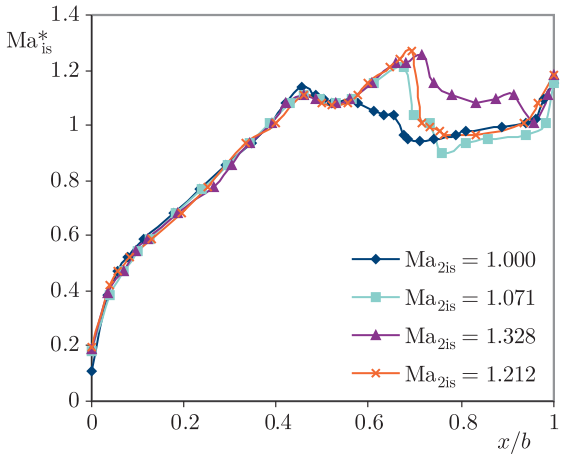

Figure 12. Distribution of Ma^*_{is} along the suction side at various Ma_{2is} and $\iota = 0°$

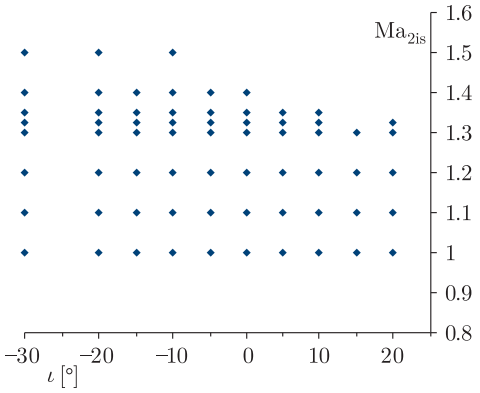

Figure 13. Regimes with shock wave – laminar boundary layer interaction

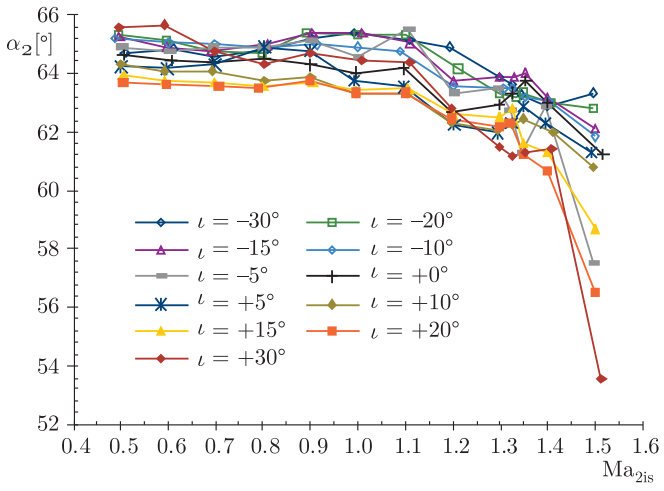

Figure 14. Dependence of exit flow angle α_2 upon Ma_{2is} and ι

the difference between the velocity on the blade's suction and pressure sides at the trailing edge is larger and so is the deflection.

3.4. Losses

Losses have been evaluated in terms of loss coefficient ζ defined as:

$$\zeta = 1 - \frac{\mathrm{Ma}_2^{*2}}{\mathrm{Ma}_{2\mathrm{is}}^{*2}}. \tag{1}$$

Its dependence on the exit Mach number is shown in Figure 15.

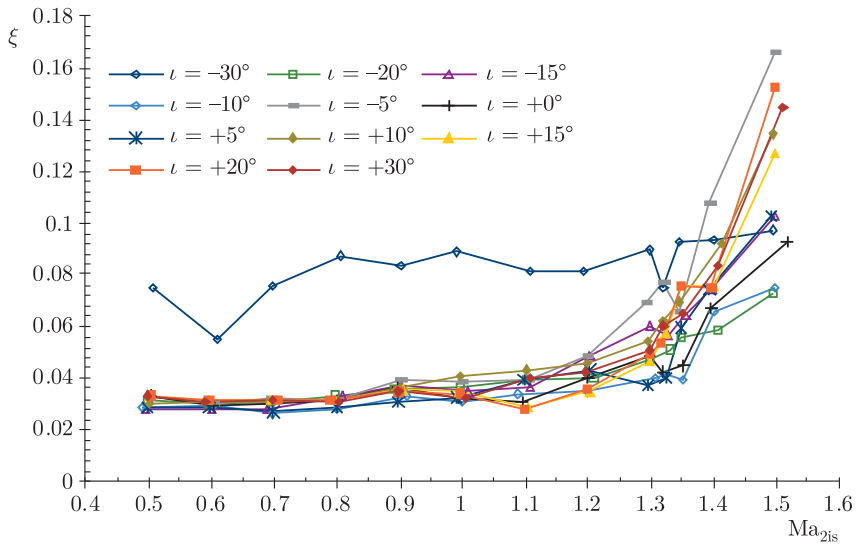

Figure 15. Dependence of loss coefficient ζ upon $\mathrm{Ma}_{2\mathrm{is}}$ and ι

It is evident that the structure causing the highest loss of kinetic energy at regimes with the exit Mach numbers of $\mathrm{Ma}_{2\mathrm{is}} \leq 1.35$ is the flow separation described in paragraph 3.1. This structure has appeared at all exit Mach numbers at the incidence angle of $\iota = -30°$ and caused an additional loss of 6% comparing to other cases of incidence angles. However, as the exit Mach number grows, a contribution of loss due to shock structures becomes larger. This contribution to loss depends on the angle of incidence and its value ranges from 0% in case of $\iota = -30°$ to 10% in case of $\iota = +30°$ at regimes with $\mathrm{Ma}_{2\mathrm{is}} = 1.5$. The large contribution value at high positive angles of incidence occurs as a result of a large difference between the velocities on the blade's suction and pressure sides at the trailing edge. The difference of velocities is governed by the exit shock wave reflection.

4. Conclusion

A series of flow field pictures and pneumatic measurements has helped to describe the behaviour and occurrence of several phenomena taking place in the transonic flow past the midsection blade cascade. We have observed a flow separation at an extreme negative angle of incidence of $\iota = -30°$ producing an additional loss of 6% at all exit Mach numbers. The mechanism of supersonic compression at transonic

expansion taking place at all transonic regimes has been observed and described. Three different ways of oblique exit shock reflection from the neighbouring blade's suction side have been documented. In particular, the principle of Mach reflection and the shock wave – laminar boundary layer interaction have been described. The presence of the reflection has been found crucial concerning the losses as the value of losses at regimes with high exit Mach numbers has increased about 10% due to a large difference between the velocities on the suction and pressure sides at the trailing edge in cases without the reflection, *i.e.* cases with a high positive angle of incidence.

Acknowledgements

The authors would like to express their thanks to ŠKODA POWER a.s. which has proposed and supported this research, to the Czech Science Foundation which has supported this research under Grant No. 101/07/1508 and to the Ministry of Education, Youth and Sport of the Czech Republic which has supported this research under Research Plan AVOZ20760514.

References

[1] Šafařík P 1997 *Proc. 13th Symposium on Measuring Techniques for Transonic and Supersonic Flow in Turbomachines*, ETH Zurich, **20**, pp. 0–14
[2] Amecke J and Šafařík P 1995 *Data Reduction of the Wake Flow Measurements with Injection of an Other Gas*, Forschungsbericht DLR 95–32, Göttingen
[3] Luxa M, Synáč J, Šafařík P and Šimurda D 2007 *Steam Turbines and Other Turbomachinery*, pp. 4/1–4/8
[4] Šťastný M and Šafařík P 1990 *ASME Paper*, New York, **90-GT-313**
[5] Shapiro A H 1954 *The Dynamics and Thermodynamics of COMPRESSIBLE FLUID FLOW*, Ronald Press, New York
[6] Dvořák R 1987 *Internal Aerodynamics*, Editorial Centre ČVUT, Prague (in Czech)